Asian Journal of Andrology (2024) 26, 484–489
www.asiaandro.com; https://journals.lww.com/ajandrology

Open Access

ORIGINAL ARTICLE

Male Infertility

Novel mutations in *LRRC23* cause asthenozoospermia in a nonconsanguineous family

Song-Xi Tang[1,*], Si-Yu Liu[2,*], Hong Xiao[1], Xin Zhang[3], Zhuang Xiao[3], Shan Zhou[1], Yi-Lang Ding[1], Peng Yang[1], Qiang Chen[1], Hai-Lin Huang[1], Xi Chen[1], Xi Lin[4], Hui-Liang Zhou[1], Ming-Xi Liu[2]

The cause of asthenozoospermia (AZS) is not well understood because of its complexity and heterogeneity. Although some gene mutations have been identified as contributing factors, they are only responsible for a small number of cases. Radial spokes (RSs) are critical for adenosine triphosphate-driven flagellar beating and axoneme stability, which is essential for flagellum motility. In this study, we found novel compound heterozygous mutations in leucine-rich repeat-containing protein 23 (*LRRC23*; c.1018C>T: p.Q340X and c.881_897 Del: p.R295Gfs*32) in a proband from a nonconsanguineous family with AZS and male infertility. Diff-Quik staining and scanning electron microscopy revealed no abnormal sperm morphology. Western blotting and immunofluorescence staining showed that these mutations suppressed *LRRC23* expression in sperm flagella. Additionally, transmission electron microscopy showed the absence of RS3 in sperm flagella, which disrupts stability of the radial spoke complex and impairs motility. Following *in vitro* fertilization and embryo transfer, the proband's spouse achieved successful pregnancy and delivered a healthy baby. In conclusion, our study indicates that two novel mutations in *LRRC23* are associated with AZS, but successful fertility outcomes can be achieved by *in vitro* fertilization-embryo transfer techniques.

Asian Journal of Andrology (2024) **26**, 484–489; doi: 10.4103/aja202435; published online: 26 July 2024

Keywords: asthenozoospermia; LRRC23; male infertility; whole exome sequencing

INTRODUCTION

Infertility is a prevalent concern that affects numerous couples globally. Male factors account for approximately 30%–50% of all infertility cases.[1–3] Asthenozoospermia (AZS) is characterized by reduced sperm motility (total motility <40% or progressive motility <32%), which arises from a combination of genetic and environmental factors.[4] Despite the genetic component commonly observed in a small number of severe AZS patients, the precise mechanisms and pathogenesis of this condition remain unclear in most cases.[5,6]

Flagella are microtubule-based organelles with a conserved structural design essential for the movement of male gametes.[7] Their principal structure is defined by a 9 + 2 axoneme pattern with nine outer doublet microtubules (DMTs) arrayed around a central pair (CP) of microtubules. Radial spokes (RSs) are T-shaped multiprotein complexes that link the CP and DMTs, transmitting mechanochemical signals vital for axoneme stability and flagellum motility.[8] Working in concert with outer arm dynein (OAD) and inner arm dynein (IAD), RSs are indispensable for adenosine triphosphate (ATP)-driven flagellar beating. In humans and mice, mutations or deletions of RS components can result in AZS and male infertility, underscoring the critical role played by RSs in flagellar motion.[9–11]

Leucine-rich repeat-containing protein 23 (LRRC23) maintains the structural integrity and functionality of sperm flagella. Zhang *et al.*[12] showed that knockout of *Lrrc23* in mice leads to an abnormal RS structure and reduced sperm motility, while ciliary beating is largely unaffected. Currently, only two studies have reported *LRRC23* gene mutations in humans.[13,14] Li *et al.*[13] reported a case in which the parents of the proband were in a consanguineous marriage and conceived their biological child through intracytoplasmic sperm injection (ICSI). Another study[14] identified two cases of *LRRC23* mutations in a consanguineous family without detailing reproductive outcomes. Further research on *LRRC23* is crucial to advance our understanding of its role in sperm motility and potential effect on male fertility.

In this study, we identified two novel compound heterozygous mutations in *LRRC23*, leading to AZS in a nonconsanguineous family. Functional analysis confirmed the pathological nature of these novel mutations. Additionally, we meticulously analyzed the clinical outcomes of assisted reproductive technologies for the patient's partner, allowing accurate genetic diagnosis for the patient and broadening the spectrum of known *LRRC23* mutations.

PATIENTS AND METHODS

Patient information

We performed whole exome sequencing (WES) of peripheral blood samples from 42 infertile males with idiopathic AZS but without obvious sperm morphological defects under an optical microscope,

[1]Department of Andrology and Sexual Medicine, First Affiliated Hospital of Fujian Medical University, Fuzhou 350005, China; [2]State Key Laboratory of Reproductive Medicine and Offspring Health, The Affiliated Taizhou People's Hospital of Nanjing Medical University, Taizhou School of Clinical Medicine, Nanjing Medical University, Nanjing 211166, China; [3]State Key Laboratory of Reproductive Medicine and Offspring Health, Department of Histology and Embryology, School of Basic Medical Sciences, Nanjing Medical University, Nanjing 211166, China; [4]Public Technology Service Center Fujian Medical University, Fuzhou 350108, China.
*These authors contributed equally to this work.
Correspondence: Dr. MX Liu (mingxi.liu@njmu.edu.cn) or Dr. HL Zhou (zhlpaper@fjmu.edu.cn)
Received: 29 December 2023; Accepted: 16 April 2024

who were recruited from the First Affiliated Hospital of Fujian Medical University (Fuzhou, China) between December 2020 and June 2023. Among these cases, one had compound heterozygous variants in *LRRC23*. The 30-year-old male, married since 2017, and his 25-year-old partner experienced infertility despite regular unprotected intercourse with subsequent examinations showing no reproductive abnormalities in the spouse. The patient presented with normal male secondary sexual characteristics, peripheral blood chromosome karyotype, and sex hormone levels without any clinical phenotypes associated with primary ciliary dyskinesia (PCD) or anatomical abnormalities. Two consecutive semen analyses within 3 months showed decreased sperm progressive motility, overall normal morphology, and total counts (**Table 1**).

This study was conducted in accordance with the relevant guidelines and regulations (Declaration of Helsinki). Written informed consent was obtained from all participants. Ethical approval was granted by the Reproductive Research Ethics Committee of the First Affiliated Hospital of Fujian Medical University (Fuzhou, China; Approval No. MRCTA, ECFAH of FMU [2022]191). The data that support the findings of this study are available from the corresponding author upon reasonable request. Some data may not be made available because of privacy or ethical restrictions.

Diff-Quik Romanowsky stain of sperm

Sperm morphology was determined by Diff-Quik staining (No. 20140076; Yue Shenzhen Medical Device Filing, Shenzhen, China). Fresh semen specimens were prepared immediately after liquefaction. After natural drying, methanol was added, and the specimen was fixed for 15 s. The specimens were stained with Diff-Quik dye I (eosin G) for 10 s. After binding to a positively charged eosinophilic protein, the cells were stained red. Subsequently, the specimen was stained with Diff-Quik dye II (thiazide dye) for 15 s, combined with negatively charged basophilic proteins, and dyed blue. The stained semen specimen was placed under running water 10–15 times, dried, and examined under a light microscope (Nikon ECLIPSE Ci-S Optical Microscope; Nikon, Tokyo, Japan).

WES and Sanger sequencing validation

To investigate potential gene mutations, we used a DNeasy Blood Kit (Qiagen, Venlo, The Netherlands) to extract genomic DNA from blood samples. WES was then performed on the proband's DNA to identify any genetic abnormalities. This involved fragmenting the DNA by Covaris-focused ultrasonication and preparing DNA sequencing libraries in accordance with the manufacturer's instructions. The Illumina NovaSeq platform (Illumina, San Diego, CA, USA) was used for sequencing with the alignment of the sequencing reads to the human genome (GRCh37/hg19) using the Burrows–Wheeler aligner. Genome Analysis Toolkit (GATK) 4.0 (Broad Institute, Cambridge, MA, USA) was employed to identify single nucleotide variants and insertions/deletions (indels) within the captured coding exonic intervals.[15] Variants were subsequently filtered and annotated using Annotate Variation (ANNOVAR) software (Open Bioinformatics Foundation, Philadelphia, PA, USA).[16] Interpretation and evidence grading followed the latest version of the American Society of Medical Genetics and Genomics Standards and Guidelines for the Interpretation of Sequence Variants.[17]

Table 1: Semen analyses of the patient with an interval of 3 months

Semen parameter	*First time*	*Second time*	*Normospermic parameters*
Ejaculate volume (ml)	3.80	2.40	≥1.50
Sperm concentration ($\times 10^6$ ml^{-1})	18.40	16.20	≥15.00
Progressive motility (%)	14.10	8.80	≥32.00
Total motility (%)	37.00	43.80	≥40.00

To validate the *LRRC23* mutations identified by high-throughput sequencing and analyze the *LRRC23* gene sequence in peripheral blood samples from the patients' parents, classic Sanger sequencing was performed. Polymerase chain reaction (PCR) amplification was carried out on each subject using specific primers (forward 1, 5'-GCGTTGGTGCTGCTTGATAA-3'; reverse 1, 5'-GCCGACTTCACTCTGTGTCA-3'; forward 2, 5'-CTTCTACCTCCAGGAGATCA-3' and reverse 2, 5'-CACAGGAGCATCACTCTGTT-3'). PCR products were subjected to bidirectional Sanger sequencing using a 3730xl DNA Analyzer (Applied Biosystems, Foster City, CA, USA).

Immunofluorescence analysis of sperm

To analyze sperm cells, the samples were spread onto slides and allowed to dry in air. The sperm cells were then fixed with 4% paraformaldehyde for 40 min. After fixation, the sperm cells were washed three times for 5 min each using phosphate-buffered saline (PBS). To retrieve antigens, the sperm cells were boiled in a microwave for 10 min in 10 mmol l^{-1} citrate buffer (pH 6.0). Following antigen retrieval, the sperm cells were washed three times with PBST (PBS containing 0.05% Tween-20) for 10 min each to remove residual debris or contaminants. To prevent nonspecific binding, the sperm cells were blocked with 5% bovine serum albumin (BSA) in PBST for 2 h, after which they were probed overnight with appropriate primary antibodies at 4°C. The generation of an antibody specific for LRRC23 has been described previously.[12] Commercial primary antibodies were as follows: anti-radial spoke head component 9 (RSPH9; 1:200; 23253-1-AP; Proteintech, Wuhan, China), anti-dynein light chain LC8-type 2 (DYNLL2; 1:200; 16811-1-AP; Proteintech), anti-NME/NM23 family member 5 (NME5; 1:200; 12923-1-AP; Proteintech), and anti-acetylated tubulin (AC-TUB; 1:500; T7451; Sigma-Aldrich, St. Louis, MO, USA). After three washes with PBST, the sperm cells were incubated for 2 h with secondary antibodies, counterstained with Hoechst 33342 (Invitrogen, Carlsbad, CA, USA) for 5 min, and then rinsed with PBST. The samples were mounted and visualized under an LSM800 confocal microscope (Carl Zeiss AG, Jena, Germany) and TCSSP8X confocal microscope (Leica Microsystems, Wetzlar, Germany).

Western blotting

Proteins were extracted from semen samples using lysis buffer (8 mol l^{-1} urea, 50 mmol l^{-1} Tris-HCl, pH 8.2, 75 mmol l^{-1} NaCl, and 2% [*v*/*w*] protease inhibitor cocktail [Roche, Basel, Switzerland]). The proteins were separated by sodium dodecyl sulfate-polyacrylamide gel electrophoresis (SDS-PAGE) in 4%–12% gradient gels and transferred onto polyvinylidene fluoride (PVDF) membranes. The membranes were blocked for 2 h with 5% dry nonfat milk in TBS with Tween-20 (TBST) at 22°C ± 2°C and then incubated with a primary antibody overnight. The generation of antibodies specific to LRRC23 and growth arrest specific 8 (GAS8) has been described previously.[12,18] Commercial primary antibodies were as follows: anti-RSPH9 (1:2000; 23253-1-AP; Proteintech), anti-DYNLL2 (1:2000; 16811-1-AP; Proteintech), anti-NME5 (1:2000; 12923-1-AP; Proteintech), and anti-β-tubulin (1:5000; AC021; Abclonal, Wuhan, China). The membranes were washed three times in TBST and then probed for 2 h with the appropriate secondary antibody. To detect protein bands, High-sig enhanced chemiluminescence (ECL) Western Blotting Substrate (Tanon, Shanghai, China) and the western blotting detection system were used.

Transmission electron microscopy (TEM)

Spermatozoa were fixed overnight at 4°C with 2.5% glutaraldehyde (Solarbio, Beijing, China). A postfixation step was then performed at 22°C ± 2°C for 1 h using a mixture of 1% osmium tetroxide and 0.5% potassium ferrocyanide in 30 mmol l^{-1} N-2-hydroxyethylpiperazine-N-2-ethane sulfonic acid (HEPES). The samples were dehydrated using an ethanol gradient and then embedded in epoxy resin at 60°C for 2 days. Ultrathin sections were prepared using an Ultracut Microtome (Leica, Berlin, Germany). The sections were stained with uranyl acetate and lead citrate and then mounted on copper grids for evaluation under a JEM-1400Flash electron microscope (JEOL, Tokyo, Japan) and FEI Tecnai G2electron microscope (FEI, Hillsboro, OR, USA).

Scanning electron microscopy (SEM)

To ensure that sperm would attach to a slide, samples were fixed at 4°C with 2.5% phosphate-buffered glutaraldehyde for 2 h. The samples were washed three times with 0.1 mol l^{-1} PBS, fixed with 1% osmium acid, and then dehydrated in an alcohol gradient ranging from 30% to 100%. The samples underwent critical point drying using a K850 Critical Point Dryer (Quorum, Letchworth, UK). A QUANTA 450 scanning electron microscope (FEI) was used to observe and image the samples.

RESULTS

WES analysis and Sanger sequencing validation

To investigate the underlying genetic factors contributing to AZS, we performed WES on the patient. Our analysis identified two variants of *LRRC23*, c.1018C>T: p.Q340X and c.881_897 Del: p.R295Gfs*32, in the proband (II:1). The transcript was NM_001135217. To further assess the pathology of these variants, we conducted targeted testing of the unaffected parents by Sanger sequencing. The results revealed that the father (I:1) carried a heterozygous nonsense mutation, whereas the mother (I:2) carried a heterozygous frameshift mutation (**Figure 1**). These findings strongly suggested that the patient inherited compound heterozygous mutations, which likely contributed to the AZS onset.

Western blotting and immunofluorescence of sperm flagellin

To further investigate the harmful effects of *LRRC23* mutations, we selected a healthy adult male of a similar age as a control. Using western blotting, we analyzed the presence of flagellar components in sperm protein extracts from both the patient and control. The results revealed an absence of LRRC23 in the patient's sperm flagella (**Figure 2a** and **Supplementary Figure 1**). To confirm this finding, we conducted immunofluorescence staining of sperm flagellar proteins, which showed that LRRC23 was normally distributed along the entire length of flagella in the control, but was completely absent in the patient's sperm flagella (**Figure 2b**).

In addition to the absence of LRRC23, we also observed a notable reduction in RS head component protein RSPH9 and RS components DYNLL2 and NME5 (**Figure 2c**–**2e**). This suggested impairment of the RS structure in the patient's sperm flagella. Additionally, we observed a tendency toward decreased expression of GAS8, a component of the nexin-dynein regulatory complex (N-DRC; **Figure 2f**).

Diff-Quik staining and SEM

After Diff-Quik staining and SEM, no observable anomalies were detected in sperm morphology. These findings suggested

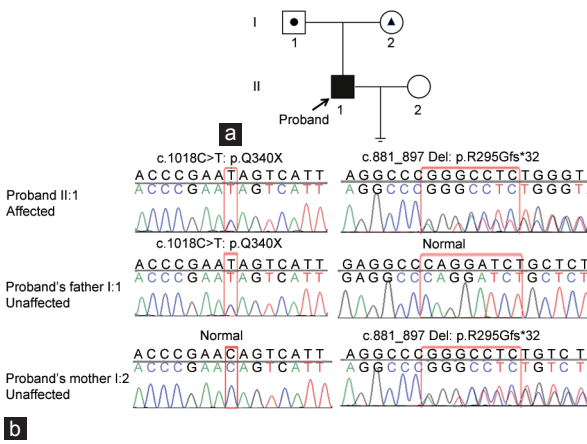

Figure 1: Biallelic mutations in *LRRC23* identified in the proband with asthenozoospermia. (**a**) Family tree of the proband with asthenozoospermia. (**b**) Sanger sequencing confirmed the biallelic mutations in *LRRC23* of the proband. Red rectangle indicates the mutation sites. *LRRC23*: leucine-rich repeat-containing protein 23.

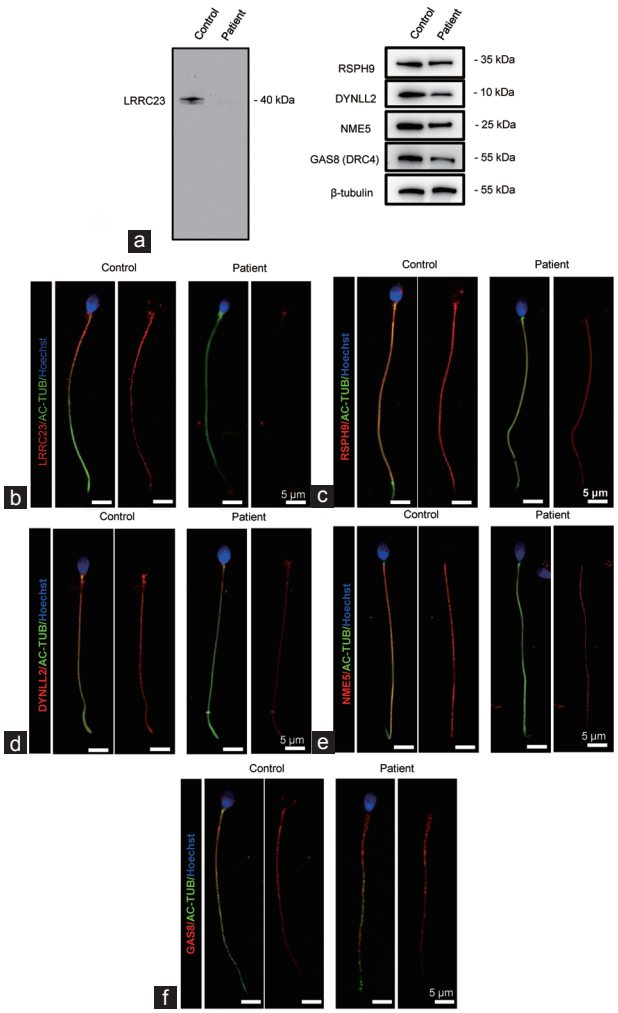

Figure 2: Absence of LRRC23 downregulates other radial spoke proteins and GAS8. (**a**) Western blotting was performed using sperm lysates from the control and patient, and antibodies against LRRC23, RSPH9, DYNLL2, NME5, GAS8, and β-tubulin. Representative immunofluorescence images of sperm from the control and patient stained with antibodies against (**b**) LRRC23, (**c**) RSPH9, (**d**) DYNLL2, (**e**) NME5, (**f**) GAS8, and AC-TUB. The nuclei of spermatozoa were labeled with Hoechst (blue). Scale bars = 5 μm. LRRC23: leucine-rich repeat-containing protein 23; RSPH9: radial spoke head component 9; DYNLL2: dynein light chain LC8-type 2; NME5: NME/NM23 family member 5; GAS8: growth arrest specific 8; AC-TUB: acetylated-tubulin.

that the size, shape, and structure of the sperm were comparable with those of normal sperm, exhibiting no discernible defects or abnormalities (**Figure 3**).

LRRC23 mutations result in an abnormal RS structure of sperm flagella

To investigate the effect of *LRRC23* mutations on sperm structure, we conducted TEM to analyze the ultrastructure of the patient's sperm flagella. TEM examination revealed abnormalities in the RS structure of the flagella. Despite the preservation of the 9 + 2 structure, we observed an irregular electron density between central and peripheral microtubules, indicating partial loss of RSs. Notably, this abnormality was consistently observed across multiple samples, ruling out the possibility of experimental artifacts. These observations indicated that *LRRC23* mutations disrupted the normal RS structure in sperm flagella (**Figure 4a**).

Sperm flagella contain the axoneme, which consists of microtubules, and the RS is a protein complex located in the axoneme. In healthy males, each 96 nm segment of the axoneme contains three RS units: RS1, RS2, and RS3. To quantitatively analyze the RS structure, we measured the grayscale intensity of three consecutive 96 nm segments (**Figure 4b**) using ImageJ software. We performed this analysis on both patient and control sperm flagella. In the control, we observed three distinct peaks in the 96 nm repeat sequence, corresponding to the signals of RS1, RS2, and RS3 with average distances between adjacent RS units of 39.04 nm, 32.64 nm, and 23.36 nm, respectively. These measurements were consistent with the expected periodic arrangement of RS. Conversely, the patient's sperm flagella showed only two peaks in the 96 nm repeat sequence with adjacent RS distances of approximately 66.02 nm and 31.41 nm (**Figure 4b** and **4c**). This suggested the absence of RS3 because the 66.02 nm gap aligned with the expected location of RS3. Importantly, the absence of RS1 or RS2 would have resulted in different gap sizes (72 nm or 56 nm, respectively). Therefore, we believed that LRRC23 played a crucial role in proper assembly of RS in sperm flagella.

Outcomes of in vitro fertilization-embryo transfer (IVF-ET)

The IVF process began with the patient providing a semen sample that was processed in the laboratory to obtain viable sperm. The retrieved 16 mature eggs from the patient's spouse were then subjected to IVF. After incubation, the fertilized eggs were checked for embryonic development and quality. A total of 10 high-quality embryos were identified. However, the initial transfer was postponed because of elevated progesterone levels in the female partner's blood. To preserve the remaining embryos, we used a vitrification procedure, which rapidly froze the embryos. A subsequent cycle was initiated, during which two of the frozen embryos were thawed and transferred via IVF to the female partner's uterus. During follow-up, embryonic cardiac activity was observed on day 25, indicating healthy development of the fetus. After a gestational period of 280 days, one healthy male infant was successfully delivered through cesarean section (**Table 2**).

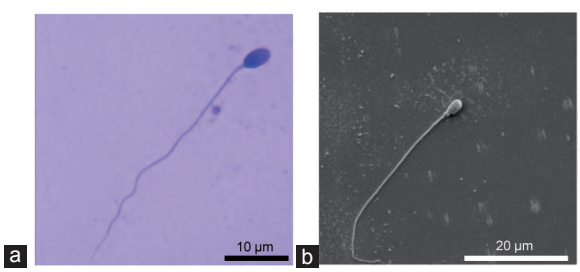

Figure 3: Diff-Quik staining and scanning electron microscopy of the proband. (**a**) Morphological analysis of sperm from the proband by Diff-Quik staining. (**b**) Observation of the proband's sperm by scanning electron microscopy.

DISCUSSION

The flagellum is essential for sperm motility and contains important structural components known as RSs. These T-shaped multiprotein complexes attached to axonemal microtubules are crucial to regulate flagellar movement of spermatozoa.[19] The integrity of RSs can significantly affect flagellar oscillations of spermatozoa, potentially affecting sperm motility and leading to male infertility.[20]

Zhang *et al.*[12] found that LRRC23 is an evolutionarily conserved protein predominantly expressed in the testis. LRRC23 is a crucial component of RSs in sperm flagella, playing an essential role in maintaining sperm motility. Hwang *et al.*[14] employed cryoelectron tomography to observe the intracellular structures of RS tri-complexes in wild-type and mutant sperm, providing evidence that LRRC23 is a head component of RS3, thereby enhancing comprehension of molecular pathological mechanisms. Male *Lrrc23* knockout mice show structural abnormalities in the sperm tail RS and decreased sperm motility, resulting in reduced penetration through the uterotubal junction.[12]

In our study, we uncovered novel compound heterozygous mutations in *LRRC23* in a patient with AZS and associated male infertility. Notably, this patient belongs to a nonconsanguineous family, contrasting earlier reports that identified *LRRC23* mutations in a consanguineous family.[13,14] Our findings underscore the relevance

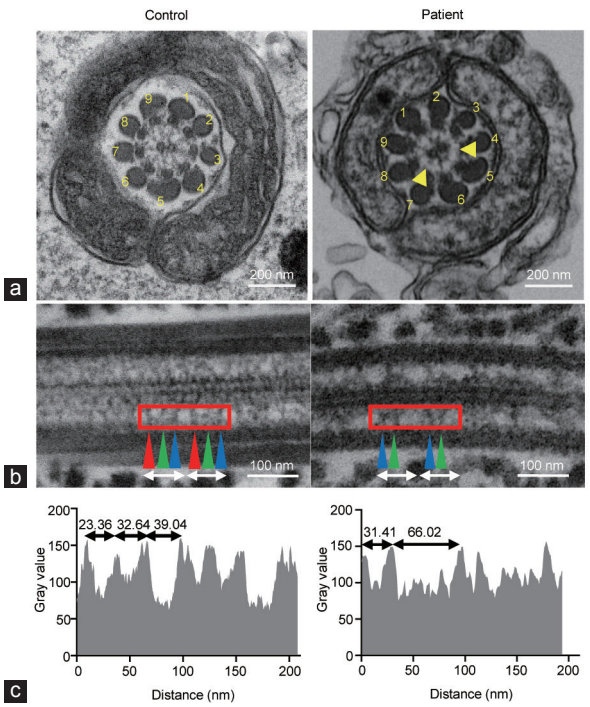

Figure 4: Ultrastructural assessment of sperm from the control and patient. (**a**) Sperm cross-sections. Outer dense fibers are represented by numbers. Missing RSs are designated by yellow arrows. Scale bars = 200 nm. (**b**) Sperm longitudinal sections. RSs (RS1–3) were arranged in 96 nm repeats in the control. In patient's flagella, RSs displayed two intact RSs with one missing RS. RS1 is indicated by the blue arrowhead, RS2 is indicated by the green arrowhead, and RS3 is indicated by the red arrowhead. Red rectangles represent the region where gray values were measured. Scale bars = 100 nm. (**c**) Distributions of gray values in the red rectangle in **b** were measured by ImageJ and plotted. RSs: radial spokes.

Table 2: *In vitro* fertilization procedure and outcome of the proband

Outcome	*Value*
Male age (year)	30
Female age (year)	25
Oocytes retrieved (*n*)	16
Fertilization rate, % (*n*/total)	81.3 (13/16)
High-quality embryo rate, % (*n*/total)	76.9 (10/13)
Embryos transferred (*n*)	2
Implantation rate, % (*n*/total)	50.0 (1/2)
Clinical pregnancy	Yes
Live birth	Boy

of *LRRC23* as a pathological factor contributing to AZS in the general population.

Using western blotting and immunofluorescence staining, we demonstrated that these mutations reduced *LRRC23* expression specifically in sperm flagella. Additionally, TEM revealed partial loss of the RS structure in sperm flagella of the patient. Further quantitative analysis using ImageJ on the axonemal structure of sperm flagella characterized the 96 nm-repeat units. In the control, we observed three distinct peaks representing RS components, whereas the patient's sperm flagella exhibited only two peaks, indicating the absence of RS3. This provides evidence of compromised RS3 integrity because of *LRRC23* mutations, a defect that likely contributes to impaired human sperm motility.

To enhance our understanding of the molecular function of LRRC23, it is crucial to identify RS-related proteins. Human RSPH9, NME5, and DYNLL2 proteins, which are orthologous to *Chlamydomonas reinhardtii* RSP9, RSP23, and RSP22, respectively, are located at the head, stalk, and base of the RS structure, respectively.[21] These proteins were chosen to comprehensively demonstrate the effect of LRRC23 on the RS structure. Our study revealed a decrease in the RS head component protein RSPH9, along with RS components DYNLL2 and NME5, indicating damage to the RS structure in sperm flagella. Furthermore, GAS8 (DRC4), a component of N-DRC, was reduced. Collectively, these observations lead us to propose that the mutations had negative effects on the expression of *LRRC23* and RS elements. Considering that an interaction between LRRC23 and RSPH9 has been reported in sperm flagella,[14] we hypothesized that a decreased interaction between LRRC23 and RSPH9 may contribute to the observed reduction in RSPH9. Nevertheless, further research is necessary to test this hypothesis.

Currently, only two studies have examined the effect of *LRRC23* gene mutations on human sperm quality, which reported reductions in sperm progressive motility, such as 9.4%, 15%, and 2% in three cases.[13,14] In our case, two consecutive semen analyses demonstrated progressive motilities of 14.1% and 8.8%. Moreover, all reported probands have displayed normal sperm concentration and morphology. Taken together, these findings suggest that mutations in *LRRC23* are linked to various degrees of AZS, ranging from nonsevere to severe without affecting the count or morphology of sperm.

In our study, the proband did not have PCD symptoms, which is consistent with previous reports in humans and mouse models.[12–14] This emphasizes a possibly distinct role of LRRC23 in the RS structure and functionality, which is specific to mammalian sperm. *LRRC23* mutation may result in RS defect-related AZS in humans without PCD symptoms, which is different from AZS linked to multiple morphological abnormalities of sperm flagella, MIP variant-associated asthenozoospermia,[22] or PCD, potentially identifying a novel etiological factor for this form of sperm motility disorder. Similar findings have been obtained with other gene mutations, such as biallelic mutations in dynein axonemal heavy chain 17 (*DNAH17*) leading to loss of the outer dynein arm in sperm flagella and causing male infertility without similar effects on respiratory cilia.[23]

Moreover, the patient's partner successfully achieved pregnancy through IVF-ET and gave birth to a healthy boy. This suggests that the *LRRC23* mutation did not affect normal embryonic development. The decision to employ IVF-ET over ICSI was based on the patient not having severe AZS because ICSI does not improve live birth rates over traditional IVF in patients with nonsevere male factors.[24] Additionally, the more invasive ICSI procedure has high costs and possibly potential health risks for the offspring. However, a previous study reported a case of successful offspring production through ICSI in an *LRRC23* proband.[13] These findings underscore the variability in manifestations of AZS caused by *LRRC23* mutations among individuals, whereas not all patients harboring *LRRC23* mutations require recourse to ICSI for embryo fertilization. However, considering the limited number of cases, further research incorporating comprehensive multicenter case analyses is imperative to determine the most effective assisted reproductive techniques for couples experiencing *LRRC23* gene-related infertility.

In summary, our study identified novel mutations in the *LRRC23* gene, leading to idiopathic AZS and male infertility by disorganizing RS3, thereby compromising the structural integrity of sperm flagella. Notably, these mutations do not interfere with embryonic development, suggesting that assisted reproduction techniques are an option for affected individuals. Our findings expand the understanding of *LRRC23* gene mutations associated with AZS and male infertility, providing valuable insights for genetic counseling and diagnosis.

AUTHOR CONTRIBUTIONS

MXL, HLZ, SXT, and SYL conceived and designed the study. SXT, HX, SZ, and HLZ contributed to the participant recruitment and characterization. SYL, XZ, and ZX conducted experiments and analyzed data. MXL assisted with the experiments and data analysis. HX, YLD, PY, QC, HLH, XC, and XL wrote the manuscript. All authors read and approved the final manuscript.

COMPETING INTERESTS

All authors declare no competing interests.

ACKNOWLEDGMENTS

We are extremely grateful to the participants for their exceptional cooperation and valuable contribution to this study. This work was supported by the National Key Research and Development Program of China (No. 2022YFC2702702), National Natural Science Foundation of China (No. 32270899 and No. 32070842), the Natural Science Foundation of Jiangsu Province (No. BK20230004), Young and Middle-Aged Key Personnel Training Project of the Fujian Provincial Health Commission (2019-ZQN-62), and Fujian Provincial Finance Project (BPB-TSX2021).

Supplementary Information is linked to the online version of the paper on the *Asian Journal of Andrology* website.

REFERENCES

1 Eisenberg ML, Esteves SC, Lamb DJ, Hotaling JM, Giwercman A, *et al*. Male infertility. *Nat Rev Dis Primers* 2023; 149: 49.
2 Fainberg J, Kashanian JA. Recent advances in understanding and managing male infertility. *F1000Res* 2019; 8: F1000 Faculty Rev-670.
3 Tournaye H, Krausz C, Oates RD. Concepts in diagnosis and therapy for male reproductive impairment. *Lancet Diabetes Endocrinol* 2017; 5: 554–64.
4 World Health Organization. WHO Laboratory Manual for the Examination and

Processing of Human Semen. 5th ed. Geneva: World Health Organization; 2010.
5 Zhou Z, Mao X, Chen B, Mu J, Wang W, *et al*. A novel splicing variant in DNAH8 causes asthenozoospermia. *J Assist Reprod Genet* 2021; 38: 1545–50.
6 Zhou Q, Xu M, Wang X, Yu M, Chen X, *et al*. Deficiency of TBL1XR1 causes asthenozoospermia. *Andrologia* 2021; 53: e13980.
7 Carvalho-Santos Z, Azimzadeh J, Pereira-Leal JB, Bettencourt-Dias M. Evolution: tracing the origins of centrioles, cilia, and flagella. *J Cell Biol* 2011; 194: 165–75.
8 Inaba K. Sperm flagella: comparative and phylogenetic perspectives of protein components. *Mol Hum Reprod* 2011; 17: 524–38.
9 Pigino G, Bui KH, Maheshwari A, Lupetti P, Diener D, *et al*. Cryoelectron tomography of radial spokes in cilia and flagella. *J Cell Biol* 2011; 195: 673–87.
10 Diener DR, Yang P, Geimer S, Cole DG, Sale WS, *et al*. Sequential assembly of flagellar radial spokes. *Cytoskeleton (Hoboken)* 2011; 68: 389–400.
11 Oda T, Yanagisawa H, Yagi T, Kikkawa M. Mechanosignaling between central apparatus and radial spokes controls axonemal dynein activity. *J Cell Biol* 2014; 204: 807–19.
12 Zhang X, Sun J, Lu Y, Zhang J, Shimada K, *et al*. LRRC23 is a conserved component of the radial spoke that is necessary for sperm motility and male fertility in mice. *J Cell Sci* 2021; 134: jcs259381.
13 Li Y, Zhang Q, Tan Q, Sha X, Gao Y, *et al*. LRRC23 deficiency causes male infertility with idiopathic asthenozoospermia by disrupting the assembly of radial spokes. *Clin Genet* 2023; 104: 694–9.
14 Hwang JY, Chai P, Nawaz S, Choi J, Lopez-Giraldez F, *et al*. LRRC23 truncation impairs radial spoke 3 head assembly and sperm motility underlying male infertility. *Elife* 2023; 12: RP90095.
15 McKenna A, Hanna M, Banks E, Sivachenko A, Cibulskis K, *et al*. The genome analysis toolkit: a mapreduce framework for analyzing next-generation DNA sequencing data. *Genome Res* 2010; 20: 1297–303.
16 Wang K, Li M, Hakonarson H. ANNOVAR: functional annotation of genetic variants from high-throughput sequencing data. *Nucleic Acids Res* 2010; 38: e164.
17 Richards S, Aziz N, Bale S, Bick D, Das S, *et al*. Standards and guidelines for the interpretation of sequence variants: a joint consensus recommendation of the American College of Medical Genetics and Genomics and the Association for Molecular Pathology. *Genet Med* 2015; 17: 405–24.
18 Zhang J, He X, Wu H, Zhang X, Yang S, *et al*. Loss of DRC1 function leads to multiple morphological abnormalities of the sperm flagella and male infertility in human and mouse. *Hum Mol Genet* 2021; 30: 1996–2011.
19 Zheng W, Li F, Ding Z, Liu H, Zhu L, *et al*. Distinct architecture and composition of mouse axonemal radial spoke head revealed by cryo-EM. *Proc Natl Acad Sci U S A* 2021; 118: e2021180118.
20 Zhang X, Xiao Z, Zhang J, Xu C, Liu S, *et al*. Differential requirements of IQUB for the assembly of radial spoke 1 and the motility of mouse cilia and flagella. *Cell Rep* 2022; 41: 111683.
21 Yang P, Diener DR, Yang C, Kohno T, Pazour GJ, *et al*. Radial spoke proteins of *Chlamydomonas* flagella. *J Cell Sci* 2006; 119: 1165–74.
22 Zhou L, Liu H, Liu S, Yang X, Dong Y, *et al*. Structures of sperm flagellar doublet microtubules expand the genetic spectrum of male infertility. *Cell* 2023; 186: 2897–910.e19.
23 Whitfield M, Thomas L, Bequignon E, Schmitt A, Stouvenel L, *et al*. Mutations in *DNAH17*, encoding a sperm-specific axonemal outer dynein arm heavy chain, cause isolated male infertility due to asthenozoospermia. *Am J Hum Genet* 2019; 105: 198–212.
24 Wang Y, Li R, Yang R, Zheng D, Zeng L, *et al*. Intracytoplasmic sperm injection versus conventional *in-vitro* fertilisation for couples with infertility with non-severe male factor: a multicentre, open-label, randomised controlled trial. *Lancet* 2024; 403: 924–34.

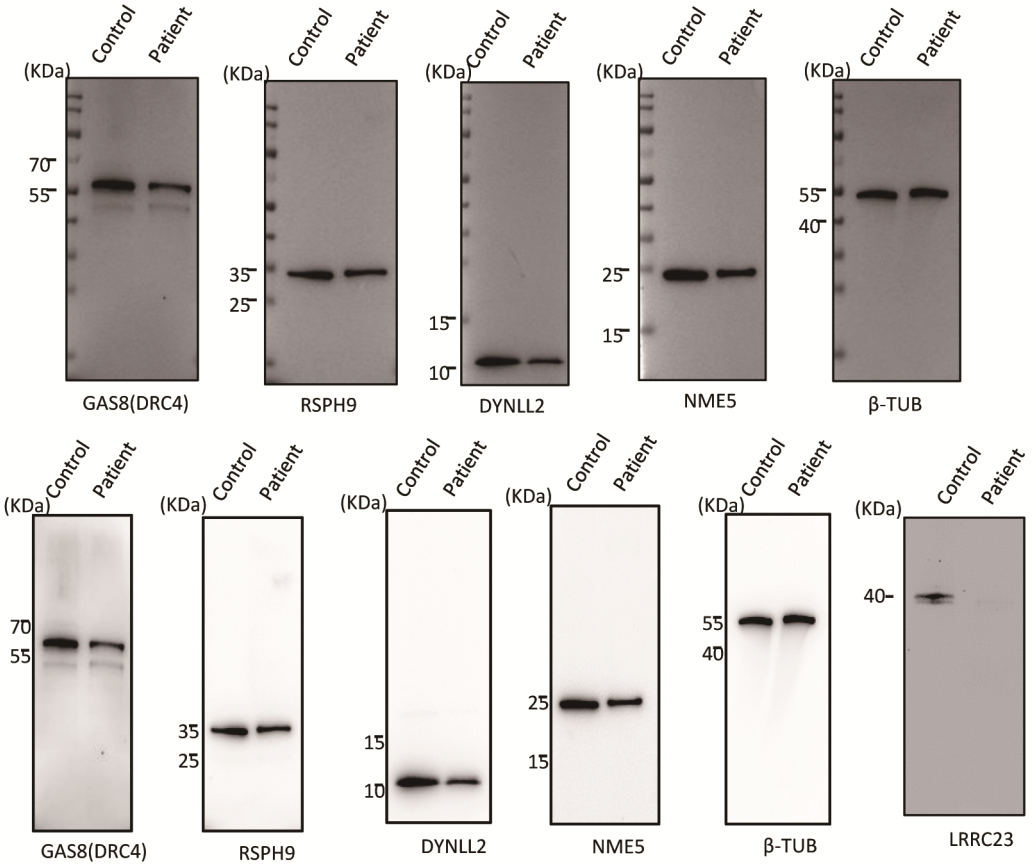

Supplementary Figure 1: Sperm flagellin levels determined by western blotting. Sperm lysates from the control and patient were subjected to immunoblotting using antibodies against LRRC23, RSPH9, DYNLL2, NME5, GAS8, and β-tubulin (β-TUB). LRRC23: leucine-rich repeat-containing protein 23; RSPH9: radial spoke head component 9; DYNLL2: dynein light chain lc8-type 2; NME5: NME/NM23 family member 5; GAS8: growth arrest specific 8; β-TUB: β-tubulin.